Available online at www.sciencedirect.com
SCIENCE DIRECT®
Journal of Organometallic Chemistry 674 (2003) 10–23
Journal of Organometallic Chemistry
www.elsevier.com/locate/jorganchem

Study of chemical structure and conjugation length in organometallic Pt(II) oligomers and polymers containing 1,4-diethynylbenzene derivatives as bridging units

I. Fratoddi [a,*], C. Battocchio [a], A. Furlani [a], P. Mataloni [b], G. Polzonetti [c], M.V. Russo [a]

[a] Department of Chemistry, University of Rome 'La Sapienza', P.le Aldo Moro 5, 00185 Rome, Italy
[b] Department of Physics, University of Rome 'La Sapienza' P.le Aldo Moro 5, 00185 Rome, Italy
[c] Department of Physics and INFM-INSTM, University of Rome 'Roma Tre', Via della Vasca Navale 84, 00146 Rome, Italy

Received 19 December 2002; accepted 10 March 2003

Abstract

The synthesis of platinum containing organometallic rigid rod oligomers and polymers, of general formula—$[PtL_2(-C\equiv C-pC_6H_4(2,5\text{-}R)_2-C\equiv C-)]_n$, where $L = PPh_3$, PBu_3; $R = H$, OC_4H_9 or $OC_{16}H_{33}$, has been carried out. The multinuclear macromolecules have been prepared by the Stille coupling in the extended one pot version. Oligomers of different chain lengths were obtained and fully characterised by means of spectroscopic techniques. Different organic spacers and precursor metal complexes have been employed in order to study and compare the reaction products. Well-defined oligomers were isolated and X-ray photoelectron spectroscopy technique provided information about the chain length and the nature of the end-groups. Luminescence and absorption studies of the newly synthesised Pt based poly-ynes are also reported. A correlation between the chain length, the nature of ligand phosphines and organic spacers with the optical properties was rationalised. The Pt metal centre played an important role in the conjugation, showing a red shift of absorption maxima upon increasing the number of repeating units. Band gaps of about 2.8–3.0 eV were found, corresponding to blue-light emission with a quantum efficiency up to about 3% for measurements performed in solution.

Keywords: Platinum poly-yne; Synthesis; Luminescence

1. Introduction

Organometallic polymers are recently gaining an increasing interest in materials science because polymeric conjugated materials, containing transition metals in the main chain or in the pendant groups [1] may display unique electric, redox and optical behaviour which make them good candidates for the development of advanced opto-electronic devices [2].

When the metal is bridged between organic conjugated spacers such as dialkynes within aromatic moieties, we are in the presence of metal–poly-ynes with a rigid rod conjugated architecture that gives rise to a number of interesting properties such as liquid crystal [3] and third order non-linear optical behaviour [4–6]. Moreover, highly ethynylated organometallic polymers have shown luminescence [7], magnetic [8] electronic [9,10] properties and their innovative characteristics are due to a synergy of delocalisation effects of the organic spacer and mobility of d metal electrons, that give rise to metal/ligand charge transfer ([11,12]) effects. These materials offer the opportunity of tailoring their physical properties by changing the transition metal and/or the organic spacer, which are the building blocks of these peculiar polymers [13].

Photoelectron spectroscopy results and theoretical calculations have shown an overlap between π occupied orbitals of the organic spacer and empty p or d orbitals of the metal in systems like $[L_nM-C\equiv C-R-C\equiv C-]_x$ [14,15]. The electronic features of model mononuclear

* Corresponding author.
E-mail address: ilaria.fratoddi@uniroma1.it (I. Fratoddi).

0022-328X/03/$ - see front matter © 2003 Elsevier Science B.V. All rights reserved.
doi:10.1016/S0022-328X(03)00156-6

complexes have been studied and the alkynyl ligands show a good σ and π donor, but low π acceptor characteristics [16]. As a consequence, only limited back-donation is expected and poly-ynic structure show band gaps around 3 eV [17]. In order to enhance π-conjugation, several research groups choose modified organic spacers with extended conjugation length, to decrease the energy of the π* molecular orbital [18] or introducing a donor atom on the spacer [19,20]. Depending on the ligand, the metal and the organic spacer, delocalisation throughout the organic moiety and the metallic centres may be enhanced [21].

From the original synthesis of Hagihara [22], a number of organometallic polymers containing metals from groups 8 to 10 have been prepared using more often square planar or octahedral coordinated precursor complexes [23,24].

A different synthetic approach was developed by Lewis and co-workers [25], and series of platinum poly-ynes have been synthesised by this way by varying the organic spacer, i.e. benzene, fluorene, thiophene etc. [26,27]. The influence of the organic spacer is reflected in the lowering of the band gap [28], while the role of the heavy metal seems to be related to a spin–orbit coupling that gives rise to efficient intersystem crossing and luminescence phenomena [29].

An alternative way to form carbon–carbon or metal–carbon bonds is the versatile Stille [30,31] reaction. In this framework we studied an extension of the Stille coupling reaction based on a one pot procedure, recently reported for poly(arylene-ethynylene) and polymetalla(arylene-ethynylene) copolymers [32,33]. In this study we applied the extended one pot (EOP) procedure to form metal–carbon bonds. It was demonstrated that also metal–iodide functionality can give rise to the formation of new bonds by coupling with stannane-acetylides [34,35] and now we applied the reaction to a metal–chloride functionality coupling with in situ distannane-protected diethynyl organic spacers.

With this aim, derivatives of 1,4-diethynilbenzene with aliphatic substituents R in position 2,5 on the aromatic ring were synthesised and the results are reported in this paper. Different aliphatic chains (R = $-OC_4H_9$, $-OC_{16}H_{33}$) were introduced in order to optimise the solubility and processability of the reaction products. The organic spacers were co-polymerised with square planar platinum complexes containing tributyl or triphenylphosphine as ancillary ligands.

The Hagihara-type dehydrohalogenation reaction was carried out between some of the organic spacers and metallic complexes in order to compare the two synthetic procedures.

Luminescence and X-ray photoelectron spectroscopy (XPS) characterisations were carried out in order to well-define the emission properties and the effective chain length. Preliminary investigations on the sensing properties of surface acoustic wave sensors based on some of the materials reported here [36,37] have raised further interest for their study and synthesis.

2. Results and discussion

2.1. Synthesis

A series of platinum poly-ynes were synthesised, namely poly-{[2,5-bis(ethynyl)benzene]-*trans*-bis(tributylphosphine)platinum(II)} **Pt–B–DEB*n*(a,b)**, poly-{[1,4-bis(ethynyl)-2,5-di(butoxy)benzene]-*trans*-bis(tributylphosphine)platinum(II)} **Pt–B–BOB*n*(a)**, poly-{[1,4-bis(ethynyl)-2,5-di(butoxy)benzene]-*trans*-bis(triphenylphosphine)platinum(II)} **Pt–P–BOB*n*(a,b)**, poly-{1,4-diethynyl-2,5-dihexadecyloxy)benzene-bis(tributylphosphine)platinum(II)} **Pt–B–HDOB*n*(a)**, and poly-{1,4-diethynyl-2,5-bis(hexadecyloxy)benzene-bis-(triphenylphosphine) platinum(II)} **Pt–P–HDOB*n*(a)**, where *n* indicates the number of platinum atoms in the chain ($n = 2$–80), and a or b the synthetic path. The molecular structures are depicted in Fig. 1.

The diethynylbenzene (DEB) monomer, already used by Hagihara was chosen as reference and the corresponding 2,5-disubstituted diethynylbenzenes, i.e. 1,4-diethynyl-2,5-bis(hexadecyloxy)benzene (BOB) and 1,4-diethynyl-2,5-bis(hexadecyloxy)benzene (HDOB) were used as organic spacers in order to study the effect of

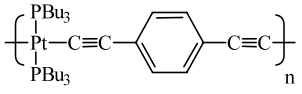

Pt-B-DEBn(a) **n= 3** terminal groups -Cl
Pt-B-DEBn(b) **n= 80** terminal groups -Cl

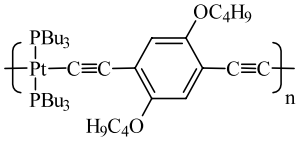

Pt-B-BOBn(a) n =2-4
terminal groups –Cl and /or $SnBu_3$

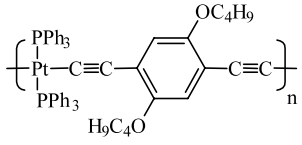

Pt-P-BOBn(a) **n =2,4**
terminal groups $SnBu_3$

Pt-P-BOBn(b) **n =12**
terminal groups -Cl

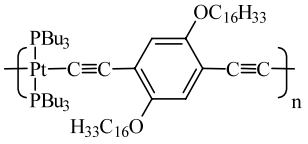

Pt-B-HDOBn(a) n =4,7
terminal groups -Cl

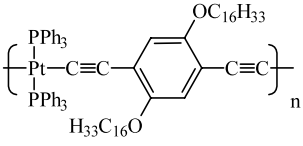

Pt-P-HDOBn(a) n= 20
terminal groups -Cl

Fig. 1. Chemical structures of Pt–poly-ynes.

both the presence and elongation of the oxyalkyl chains on solubility and reactivity.

Two synthetic pathways were compared for Pt–B–DEB*n* and Pt–P–BOB*n*, i.e. dehydrohalogenation (b) and the EOP modification of the Stille coupling reaction (a) In the dehydrohalogenation route terminal alkynes need to be prepared and isolated, before the reaction with PtL_2Cl_2 complexes, whereas in the EOP coupling, aromatic diiodides can be the reaction precursors. The conventional Stille reaction is based on a coupling, in the presence of palladium, between electrophiles and organotin reagents. Herein, we report this synthetic procedure where three consecutive steps were cumulated (see Fig. 2): 1st step) the coupling between an organic diiodide and tributyl(ethynyl)tin, is carried out in order to obtain an organic dialkyne and the iodotributyltin side-product. The coupling is carried out by overnight stirring the reaction mixture in THF at 70 °C. The mixture slowly turned from colourless to brown–orange. 2nd step) a stoichiometric amount of lithium-diisopropylamide (LDA) is directly added to this reaction mixture, previously cooled at 0 °C. This provokes the removal of the acetylenic proton from the terminal acetylenic functionalities and their immediate recombination with the Bu_3SnI with formation of the corresponding (bis)trialkyltinethynyl derivatives. The mixture changed colour with a little darkening. 3rd step) the metaldichloride complex PtL_2Cl_2 is subsequently added to this reaction mixture and formation of the polymer takes place by the palladium-catalysed coupling between the M–Cl and Bu_3Sn–C≡C– moieties.

In the case of Pt–B–DEB*n*(b) a polymeric compound was obtained by the dehydrohalogenation method from DEB and *trans*-$[Pt(PBu_3)_2Cl_2]$ as confirmed by gel permeation chromatography (GPC) measurements ($n \cong 80$ repeating units). The ^{1}H-NMR resonance of the aromatic region was found at $\delta = 7.07$ ppm, whereas the tributyl chains on the phosphinic ligand showed multiplets at $\delta = 2.09$, 1.57, 1.41 ppm (CH_2) and 0.89 (CH_3). The main resonance in the ^{31}P-NMR spectra was assessed to phosphorus atoms bonded to internal platinum units, at $\delta = 3.50$ ppm. The coupling constant $J(^{195}Pt–^{31}P)$ was typical of a *trans* geometry around the metal (~ 2360 Hz) [38]. In order to compare the two reaction paths, the Stille EOP coupling was carried out on the same precursors, and the formation of a main coupling product was observed, i.e. the trinuclear compound Pt–B–DEB3(a), which showed two ^{31}P-NMR resonances at $\delta = 3.50$ and 0.76 ppm with intensity ratio 1:2. The formation of a trinuclear

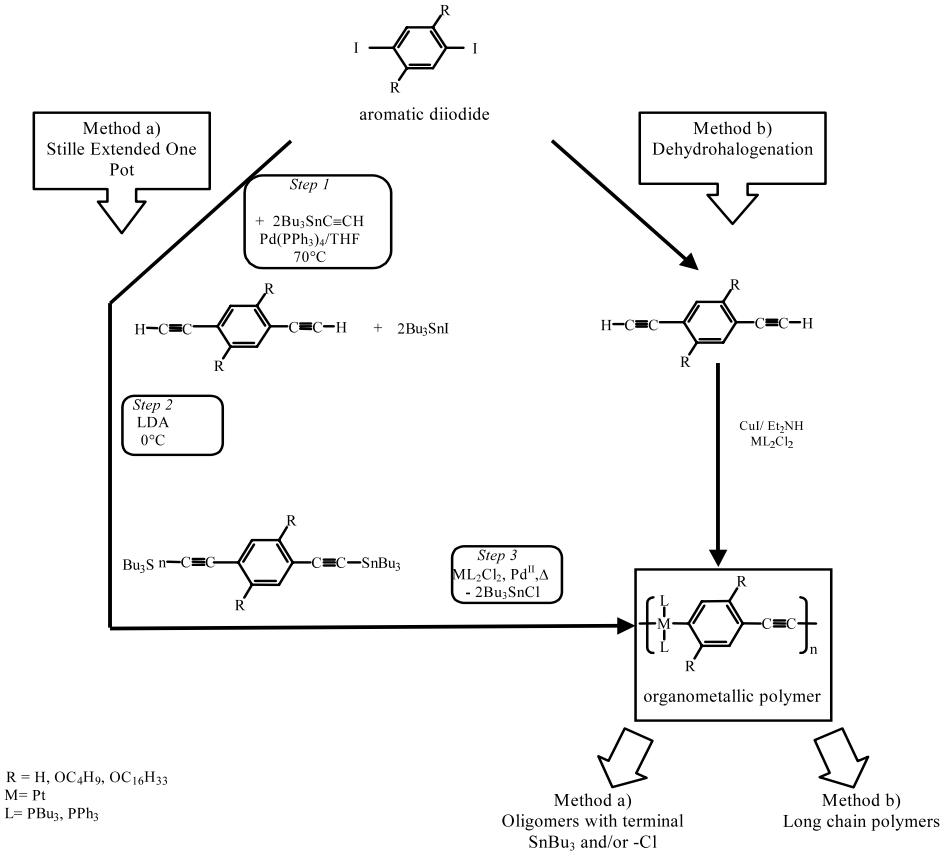

Fig. 2. Synthetic pathways: method (a) EOP Stille coupling and (b) dehydrohalogenation reaction.

compound could be assessed, as confirmed also by elemental analyses.

The studies on the two reaction methods have been extended to the reactivity of BOB monomer, by introducing alkoxyalkyl pending chains on the aromatic spacer and the chemical structure of the metal moiety by using *cis*-[$Pt(PPh_3)_2Cl_2$]. In this reaction (EOP pathway), the crude product obtained was a red oil, which was chromatographated to separate the oligomers. Two main products were isolated, i.e. dinuclear and tetranuclear compounds with terminal stannane groups, as XPS measurements and elemental analyses let us to assess. Pt–P–BOB2(a) and Pt–P–BOB4(a), showed in the ^{1}H-NMR spectra, the singlet of the aromatic protons at $\delta = 6.56$ ppm, and the $-OCH_2-$ triplet at 3.75 ppm. The resonances arising from the aliphatic region were centred at $\delta = 2.09$, 1.59, 1.35 (CH_2) and 0.90 (CH_3) ppm, as unresolved multiplets. In the case of Pt–P–BOB4(a), two ^{31}P-NMR resonances were observed, at $\delta = 18.07$ and 17.67 ppm with intensity ratio 1:1, confirming the formation of a tetranuclear compound. *Trans* geometry around the metal was assessed from the value of the coupling constant $J(^{195}Pt-^{31}P)$ of about 2600 Hz, typical of a *trans* geometry in diacetylyde-platinum complexes [39]. A *cis–trans* isomerisation occurred around the Pt centre, that is expected behaviour of *cis*-[$Pt(PPh_3)_2Cl_2$] reacting with acetylenes [40].

An oligomeric compound containing about 12 repeating units (Pt–P–BOB*n*(b)) was obtained in the case of the dehydrohalogenation reaction on the same precursors, as suggested from the ^{31}P-NMR signals intensity ratio. In fact, two main signals were found as in the previously described compound, at about 18.2 and 17.7 ppm, with intensity ratio 5:1.

In the case of DEB and BOB organic spacers, the two methods exhibit a marked difference in reactivity that is a preferential yield in long chain polymer formation in the dehydrohalogenation route, while multinuclear Pt complexes are the main products of the EOP synthetic procedure. The different length of Pt–B–DEB*n*(b) and Pt–P–BOB*n*(b) ($n = 80$ and 12, respectively) is probably due to the different phosphinic ligand that affect the solubility of the growing chain. As a general rule, PBu_3 ligand enhance the solubility of the metal complex units of the polymer.

The synthesis of π-conjugated oligomers of well-defined chemical structure is actually of interest, in view of the dramatic increase of research devoted to the synthesis of materials in the nano-scale for the new frontier of molecular electronics [41]. On the basis of our preliminary results, the studies with EOP synthetic method have been extended to BOB and HDOB monomers and Pt complexes.

In the case of Pt–B–BOB*n*(a) based materials, the EOP method gave rise to oligomeric coupling products and dinuclear, trinuclear and tetranuclear compounds were isolated. The ^{1}H-NMR spectra showed resonances of the organic spacers and of the ancillary phosphines at the same values of the already reported compounds. For Pt–B–BOB2(a), a single resonance was observed in the ^{31}P-NMR, centred at $\delta = 0.92$ ppm, whereas in Pt–B–BOB3(a) and Pt–B–BOB4(a) terminal and internal phosphines were assessed to the signals at about 0.90 and 1.00 ppm, respectively, with intensity ratios 2:1 and 1:1.

Reactions in the same experimental conditions, performed using the same Pt precursor complex with HDOB monomer, gave the Pt–B–HDOB*n*(a) based materials. The ^{31}P-NMR spectra of Pt–B–HDOB4(a) showed two resonances centred at $\delta = 0.90$ (terminal) and 0.99 (internal) ppm ($J_{Pt-P} = 2300$ and 2311 Hz, respectively), both due to the tributylphosphines bonded to platinum in a *trans* configuration. The two resonances are in 1:1 ratio as expected for a tetranuclear compound.

Pt–B–HDOB7(a) also showed two signals in the ^{31}P-NMR spectra, with the intensity ratio 2:5, (at $\delta = 0.90$ and 1.00 ppm). In this case the molecular structure is consistent with an heptanuclear compound.

When the ancillary ligand on Pt was PPh_3, we observed the formation of a red oil (Pt–P–HDOB*n*(a)). Only one signal in the ^{31}P-NMR spectrum was observed for Pt–P–HDOB*n*(a) (centred at $\delta = 18$ ppm) due to internal phosphorus atoms of a polymeric compound. This hypothesis was confirmed by GPC ($n \cong 20$) and elemental analysis (see Section 4).

Comparing these results with those relative to the compounds obtained from the BOB spacer, we observed the formation of products with longer chain length. The influence of longer alkoxy chains on the aromatic spacer, improves the solubility of the as-formed coupling products and make them more suitable for further couplings.

The GPC analysis carried out on our polymeric materials (Pt–P–BOB*n*(b), Pt–P–HDOB*n*(a), Pt–B–DEB*n*(b)) underestimates the molecular weight. In fact previously reported measurements carried out on Ni-arylenes [42], showed that the polystyrene standard, a random coil material, significatively differs from the rigid rod structure of the materials under study. A rough scale up of our GPG molecular weights was possible by the following approach. In Table 2 the GPC measurements of the organometallic compounds are compared with the values obtained for the precursor complexes *trans*-[$Pt(PBu_3)_2Cl_2$] and *cis*-[$Pt(PPh_3)_2Cl_2$]. GPC results gave $M_w = 312$ ($M_n = 310$) and $M_w = 360$ ($M_n = 320$), respectively, while the calculated molecular weights are 664.0 and 784.0 a.m.u. On the basis of these comparisons, the reported values of M_w and M_n are expected to underestimate of about one half the real molecular weights of our compounds.

Table 1
Chemical and spectroscopic characterization of Pt–poly-ynes

Sample	Elemental analyses		^{31}P-NMR [a]		IR (film) (cm^{-1})			Formula
	C% H%	(C% calc.) (H% calc.)	δ (ppm)	$J(^{31}P-^{195}Pt)$ (Hz)	ν (C≡C)	ν (Pt–Cl)	ν (C–Sn)	
Pt–B–DEB3(a)	51.71 8.17	(52.16) (8.09)	3.50 0.76	(2362) (2303)	2104	328		$C_{92}H_{170}P_6Pt_3Cl_2$
Pt–B–DEB*n*(b)	56.15 8.54	(56.42) (8.08)	3.50	(2361)	2100			$C_{34}H_{58}P_2Pt$
Pt–B–BOB2(a)	51.58 8.49	(51.52) (8.38)	0.92	(2313)	2104	326		$C_{66}H_{128}O_2P_4Pt_2Cl_2$
Pt–B–BOB3(a)	56.79 8.50	(56.58) (8.57)	0.91 0.99	(2316) (2314)	2106	328	525 540	$C_{156}H_{249}O_6P_6Pt_3SnCl$
Pt–B–BOB4(a)	58.98 8.52	(58.38) (8.63)	0.94 1.01	(2316) (2314)	2104		525 533	$C_{210}H_{370}O_{10}P_8Pt_4Sn_2$
Pt–P–BOB2(a)	63.00 5.60	(63.78) (6.20)	12.00	(3454)	2104		525 540	$C_{150}H_{174}O_6P_4Pt_2Sn_2$
Pt–P–BOB4(a)	63.95 5.74	(64.55) (5.75)	18.07 17.67	(2654) (2610)	2104		528 540	$C_{258}H_{274}O_{10}P_8Pt_4Sn_2$
Pt–B–HDOB4(a)	63.00 9.70	(62.23) (9.88)	0.90 0.99	(2300) (2311)	2104	327		$C_{222}H_{420}O_6P_8Pt_4Cl_2$
Pt–B–HDOB7(a)	64.02 9.91	(63.86) (10.03)	0.90 1.00	(2300) (2311)	2109	327		$C_{420}H_{786}O_{12}P_{14}Pt_7Cl_2$
Pt–P–BOB*n*(b)	66.12 5.13	(65.64) (5.10)	18.18 17.67	(2682) (2610)	2099			$C_{54}H_{50}O_2P_2Pt$
Pt–P–HDOB*n*(a)	71.20 7.31	(70.72) (7.46)	18.00	(2595)	2106			$C_{78}H_{78}O_2P_2Pt$

[a] ^{31}P-NMR spectra (in $CDCl_3$) are referred to H_3PO_4 85%.

Table 2
Molecular weights of Pt–poly-ynes determined by GPC

Sample	M_w	M_n	*n* [a]	Repeating unit [b] (pm)
$[PtCl_2(Pbu_3)_2]$	312	310		$C_{24}H_{54}Cl_2P_2Pt$ (664.00)
$[PtCl_2(PPh_3)_2]$	360	320		$C_{36}H_{30}Cl_2P_2Pt$ (784.00)
Pt-B–DEB*n*(b)	57000	18000	80–25	$C_{34}H_{58}P_2Pt$ (723.85)
Pt–P–BOB*n*(b)	7700	3200	8–3	$C_{54}H_{50}O_2P_2Pt$ (988.00)
Pt–P–HDOB*n*(a)	26700	15800	20–12	$C_{78}H_{98}O_2P_2Pt$ (1324.64)

[a] *n*, number of r.u.
[b] Calculated molecular weight of r.u.

2.2. Optical absorption and emission studies

A growing interest in different research areas has risen for the use of organic materials as active layers in luminescence based devices. The use of conjugated polymers was deeply investigated for the advantages of ease of fabrication and low cost, but the number of materials effectively used is still limited. In fact solubility and high luminescence efficiency, required for practical applications, are usually very difficult to achieve.

Photoluminescence (PL) and electroluminescence (EL) studies give information about the nature of the excited states [43], a basis for the interpretation of the behaviour of EL devices.

Pt–B–BOB*n*(a), Pt–P–BOB*n*(a), Pt–B–HDOB*n*(a) and Pt–P–HDOB*n*(a) oligomers of different chain length (2–7 units) were investigated by absorption spectroscopy and experimental data are collected in Table 3. Spectra recorded both in solution or thin solid films, showed similar absorption maxima and shapes indicating negligible complex/solvent interaction.

The spectra of organometallic compounds displayed $\pi-\pi^*$ absorption bands red shifted with respect to the organic monomeric precursors, and the red shift increased by increasing the number of repeating units going from about 360 to 390 nm, as shown in Fig. 3. The oligomers showed a bathocromic shift absorption (nearly 40 nm) by comparison with the absorption maxima of BOB ($\lambda = 335.2$ nm) and HDOB ($\lambda = 332.6$ nm). This effect is indicative of an electronic delocalisation occurring through the Pt centres, involving a contact between the π orbitals of the organic conjugated spacer with the Pt 5d and 6p orbitals as discussed by Lewis and co-workers [44]. A further evaluation of the delocalisation effect can be estimated from the IR ν(C≡C) and ν(M–C) stretching modes [45]. $\prod$-delocalisation induces a structural variation from alkyne to allene that can be revealed by a shift towards lower frequency for the ν(C≡C) and to higher frequency for the ν(M–C)

Table 3
Optical characterization of Pt–poly-ynes: UV–vis and luminescence in $CHCl_3$ solution or thin film

Sample	λ_{abs} max. (nm)		ε_0 ($l\,mol^{-1}\,cm^{-1}$)	E_g (eV)		λ_{em} max. (nm)		η (%)
	Solution	Film		Solution	Film	Solution	Film	
Pt–B–BOB2(a)	368.0	365.4	2.03×10^4	3.20	3.20	470.0	440.0	0.25
Pt–B–BOB3 (a)	377.0	371.8	7.64×10^4	2.80	2.75	465.0 445.0	440.0	0.35
Pt–B–BOB4(a)	389.0	387.2	1.41×10^5	2.75	2.25	470.0	440.0 425.0	0.85
Pt–P–BOB2(a)	389.0	387.8	1.96×10^4	2.90	2.80	470.0	440.0	0.11
Pt–P–BOB4(a)	396.0	398.2	3.46×10^4	2.80	2.75	460.0	440.0	0.30
Pt–B–HDOB4(a)	377.0	[a]	5.30×10^4	2.95	[a]	450.0 427.0	[a]	2.33
Pt–B–HDOB7(a)	380.0	376.4	6.38×10^5	2.90	2.30	460.0 430.0	440.0 420.0	3.16

[a] The complex exhibits films of poor optical quality.

stretching modes. In our case a value of about 2100 cm^{-1} was found for ν(C≡C) in all the investigated materials, lowered with respect to the organic monomers by about 40 cm^{-1}. This trend can be associated with the presence of a higher conjugation degree in the coupled products.

These observations may be correlated with the presence of the valence shell orbitals of the transition metal conjugated with the π-system of the organic spacers, as theoretically expected [46]. According to literature report [47], the absorption peak may be associated with the $S_0 \rightarrow S_1$ transition from the highest occupied molecular orbital (HOMO) to the lowest unoccupied molecular orbital (LUMO), which are delocalised π and π* orbitals.

The HOMO–LUMO energy gap E_g was estimated from the absorbance vs. eV spectra, recorded for both solution and thin film samples. Values in the range 2.8–3.2 eV, in analogy with literature data [48], were observed. However, it is noteworthy that the E_g values decreased by increasing the number of platinum units. E_g values similar were found for oligomers of the same chain length, by varying the aliphatic chains on the organic spacer or the phosphine ligands. The variation of the ancillary phosphines on the metal and of the aliphatic chains does not significantly affect the energy of HOMO and LUMO molecular orbitals, as expected.

Luminescence spectra were recorded for solutions and thin films, and relative quantum yields η were calculated. In analogy with absorption spectra, luminescence features of films and solutions showed strong similarities. The luminescence of our materials is in the blue–green region of the visible spectrum, with peaks ranging from $\lambda_{em} = 430$–470 nm (see Table 3). The emission features are shifted to longer wave-lengths on going from monomers ($\lambda_{em} = 392$ (HDOB) and 387 nm (BOB)) to multinuclear compounds and a rise of η with increasing the molecular weight was observed. The

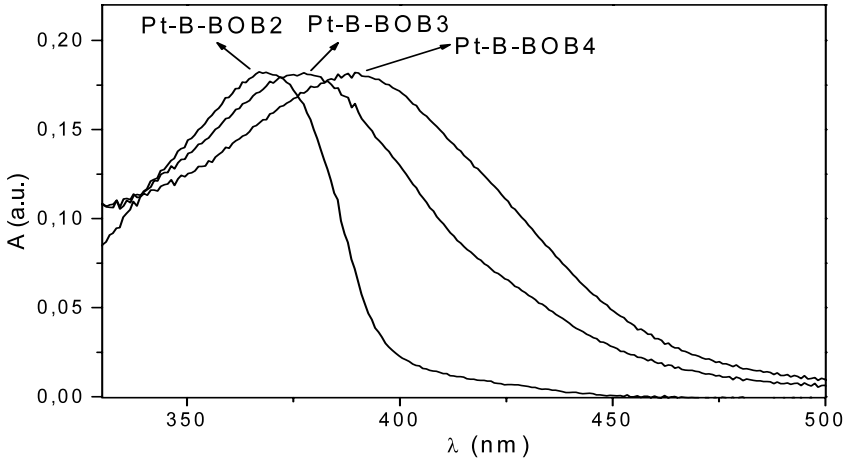

Fig. 3. UV–vis absorption spectra of Pt–B–BOB2-3-4 in $CHCl_3$ solution.

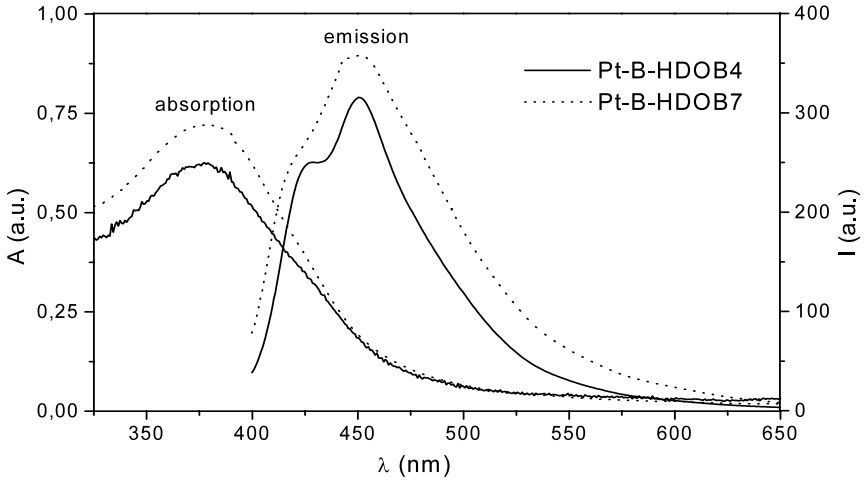

Fig. 4. UV–vis absorption and emission spectra of Pt–B–HDOB4 and Pt–B–HDOB7 in $CHCl_3$ solution.

well-resolved spectra exhibited two peaks, while broad emission features were found in some cases (Table 3). The peak at lower wave-length (~ 440 nm) is assigned to the emission due to a singlet excited state (S_1–S_0 fluorescence) and the second one (ca. 470 nm) to the emission from a triplet excited state (T_1–S_0 phosphorescence) in agreement with the literature [49]. A method to ascertain the attribution of emission features (fluorescence and phosphorescence) was developed by chemical doping of our materials with molecular iodine. In analogy with other π-conjugated materials, a redox-based charge transfer reaction may affect the π–π* electronic transition [50], with formation of a polyiodide molecule according to the reaction reported as an example: $3I_2 + 2Pt{-}B{-}HDOB4 \rightarrow 2Pt{-}B{-}HDOB4^+ + 2I_3^-$. In our case the reaction with I_2 led to a quenching of the fluorescence peak (S_1–S_0) at about $\lambda_{em} = 430$ nm, whereas the phosphorescence peak at about $\lambda_{em} = 450$ nm remained unchanged. In order to unambiguously attribute these peaks, measurements of half lifetime of the excited states by means of time-resolved measurements will be performed.

The emission spectra, measured in solution, of the oligomers showed an increase of quantum yield by increasing the number of Pt centres (Table 3). Oligomers Pt–B–HDOB*n*(a), which have the organic spacer with longer aliphatic chain ($OC_{16}H_{33}$), showed higher emission intensity and relative quantum yield (3.16% for Pt–B–HDOB7(a)) in comparison with the same oligomers with BOB spacer (shorter aliphatic chain OC_4H_9). In Fig. 4 luminescence and absorption spectra of Pt–B–HDOB4(a) and Pt–B–HDOB7(a) are reported. As it can be seen, a difference between absorption and emission maxima of about 70–80 nm was found and the highest quantum efficiency was observed in Pt–B–HDOB7(a) sample, suggesting a role, not obvious, of the ancillary ligand phosphines.

2.3. X-ray photoelectron spectroscopy

The actual interest in oligomers, which exhibit most of the relevant properties of the corresponding polymers, prompted us to investigate in depth the electronic structure of our Pt-based oligomers with BOB and HDOB organic spacers by means of XPS technique. The C1s, O1s, Pt4f, P2p, Cl2p and Sn3d core level spectra of the oligomers of different length were acquired and a summary of the core level binding energies (BE) and full width at half maximum (FWHM) values is reported in Table 4.

The C1s spectra of all our samples appeared structured and could be deconvoluted by curve fitting into three individual peaks assigning the main feature at BE = 285.0 eV to aromatic carbon (triphenylphosphine containing samples) or the peak at BE = 284.7 eV to the carbons of tributylphosphine based compounds. The asymmetries in the C1s peak are due to the carbons bonded to less electronegative atoms (≡C–Pt, C–Sn), and to carbon atoms bound to oxygen (C–O), in all the oligomers. As an example the C1s signal of Pt–B–HDOB7(a) is reported in Fig. 5a, where the main C1s peak is found at BE = 285.0 eV, the C–Pt signal at 283.7 eV and C–O at BE = 286.4 eV.

The P2p spectra show binding energy values of about 131.0 eV consistent with those measured for metal-bonded phosphine groups, in agreement with the values reported in the literature [51].

The analysis of Pt4f spectra provided some useful information on the effect of the conjugation length of the organometallic system on the charge distribution. The BE values of the $Pt4f_{7/2}$ component of different oligomers and of the inorganic starting complexes were compared in order to find a correlation between the position of the $Pt4f_{7/2}$ peak and the length of the rod-like molecule. From the observed trend of the data (see

Table 4
XPS measurements of Pt–poly-ynes: BE values for core levels and atomic ratios (in parenthesis calculated ratios)

Sample	C1s		$Pt4f_{7/2}$ BE (eV)	$P2p_{3/2}$ BE (eV)	$Cl2p_{3/2}$ BE (eV)	$Sn3d_{5/2}$ BE (eV)	n° Cl/Pt		n° Sn/Pt	
	BE (eV)	FWHM					Exp.	(Calc.)	Exp.	(Calc.)
Pt–B–BOB2(a)	285.0 283.5 286.7	1.82	72.3	131.0	199.2		0.89	(1.0)		
Pt–B–BOB3(a)	285.0 283.5 286.5	1.77	72.5	131.1	199.3	486.9	0.28	(0.33)	0.38	(0.33)
Pt–B–BOB4(a)	285.0 283.3 286.5	1.82	72.1	130.8		486.1			0.48	(0.5)
Pt–P–BOB2(a)	284.7 283.4 286.2	1.86	72.4	131.3		486.3			0.97	(1.0)
Pt–P–BOB4(a)	284.7 283.1 286.2	1.87	72.1	131.6		486.5			0.41	(0.5)
Pt–B–HDOB4(a)	285.0 283.3 286.4	1.70	72.6	131.4	199.2		0.46	(0.5)		
Pt–B–HDOB7(a)	285.0 283.7 286.4	1.80	72.1	131.1	199.3			0.28	(0.29)	
$[Pt(PPh_3)Cl_2]$	284.7		73.3	131.3	198.4					
$[Pt(PBu_3)Cl_2]$	285.0		73.4	131.8	199.1					

Table 4), it comes out that the transition metal favours the conjugation through the organometallic system. The d and p atomic orbitals of the metal are, at least in part, involved in the delocalisation of π electrons of the organic spacers. In fact, the $Pt4f_{7/2}$ binding energy in the precursor square planar complexes *trans*-$[Pt(PBu_3)_2Cl_2]$ and *cis*-$[Pt(PPh_3)_2Cl_2]$ are 73.4 and 73.3 eV, respectively, as already reported in the literature [52]; while the lower BE values measured in our samples indicated that Pt atoms have an increased electron density. However, the $Pt4f_{7/2}$ BE values for oligomers of different length ($n =$ 2–7) are relatively close to each other, suggesting a charge distribution that tends to an average extent (Fig. 5b).

Photoelectron spectroscopy measurements provided useful information for a complete characterisation of terminal groups of the here investigated multinuclear oligomers. The analysis of the Cl2p and Sn3d spectra allowed to identify the chloride or $SnBu_3$ ending groups; in fact from the synthetic pathway showed in Fig. 2, it is possible to obtain compounds with terminal chloride or $SnBu_3$ moieties.

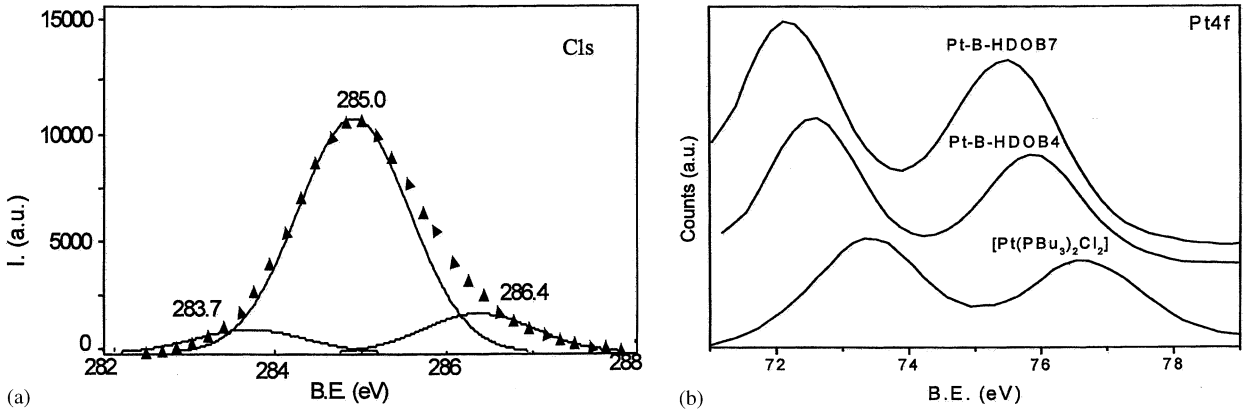

Fig. 5. C1s and Pt 4f core level spectra of Pt–B–HDOB7.

The Cl2p BE values for Pt–B–HDOB*n*(a) and Pt–P–BOB*n*(a) were found in the range 198.0–199.0 eV, consistent with chlorine bonded to a metal atom; similar values have been reported for Pt-complexes [53,54]. The presence of $SnBu_3$ terminal groups was also stated by the analysis of the $Sn3d_{5/2}$ XPS signal with a BE value at 486.5 eV. This signal is attributed to a Sn atom bonded only to carbon atoms [55], as expected for $-C\equiv C-SnBu_3$ moieties.

The evaluation of Pt/Cl and Pt/Sn atomic ratios was fundamental in the assessment of the chemical structure of the systems, the presence of these elements being strictly connected to the terminal groups, and therefore giving a reasonable estimate of the number of Pt(phosphine)$_2$ units in the chains, then yielding the oligomers length.

The XPS data provided results in good agreement with the molecular structures suggested by other techniques, i.e. ^{31}P-NMR and elemental analysis. IR spectroscopy also confirmed the nature of ending groups, showing the Pt–Cl stretching mode at about 340 cm^{-1} in those oligomers where appreciable chlorine XPS signal was found, and C–Sn stretching modes at 525 and 540 cm^{-1} in those samples having XPS Sn3d signal.

Hereafter, the most significative results concerning Pt–B–HDOB4(a) and Pt–B–HDOB7(a) will be discussed, as these macromolecules are representative of different series and show the best optical properties. The analysis of Pt–B–HDOB*n*(a) materials showed the presence of chlorine terminal groups. In this case the presence of chlorine atoms was observed at BE value 199.2 eV typical of a Cl–Pt moiety, as confirmed also by IR spectrum, where the Pt–Cl stretching band was found at 327 cm^{-1}. Evaluation of the XPS atomic ratios (Cl/Pt = 0.46), comparison with elemental analyses results and ^{31}P-NMR spectra, allow to conclude that the chemical structure of this compound is corresponding to a tetranuclear complex, as depicted in Fig. 6.

The C1s signal of the aliphatic carbon atoms was calibrated at 285.0 eV, showed asymmetries arising from carbon atoms bonded to platinum and to oxygen (Table 4), as already discussed.

The $Pt4f_{7/2}$ main signal of Pt–B–HDOB4(a) was centred at 72.6 eV, shifted of about 0.8 eV to the low BE side from the corresponding signal found for the *trans*-[$Pt(PBu_3)_2Cl_2$] precursor (see Table 4). This increased charge density at the Pt atoms indicates the occurrence of electron communication throughout the metal and the organic spacers.

The $P2p_{3/2}$ signal found at 131.4 eV, appears unmodified with respect to the pristine complex, and with a Pt/P ratio of 0.5 as expected.

The C1s signal of Pt–B–HDOB7(a) sample can be deconvoluted into three components, at 285.0, 283.7 and 286.4 eV, respectively, due to C–C, C–Pt and C–O contributions (Fig. 5a). The $Pt4f_{7/2}$ signal was found at 72.1 eV, shifted by about 1.3 eV from the starting platinum complex, indicating an enhanced electronic charge transfer from the organic spacer to the Pt centre. Evaluation of the Cl/Pt intensity ratio that is 0.28, leads to the assessment of a molecular structure corresponding to an heptanuclear complex, result that is also supported by the elemental analyses and ^{31}P-NMR results.

3. Summary

Highly ethynylated polynuclear Pt(II) complexes, with metal centres linked through 1,4-diethynyl-2,5 alkoxyalkyl benzenes have been synthesised by using the EOP route. Organometallic oligomers with variable chain length and terminal groups have been characterised with XPS and NMR investigations. The presence of Cl or $SnBu_3$ ending groups represents a chance to prepare materials with tailored chain length by applying the building block approach, as an extension of this research. The dehydrohalogenation route, performed by comparison in few cases, leads to polymeric materials.

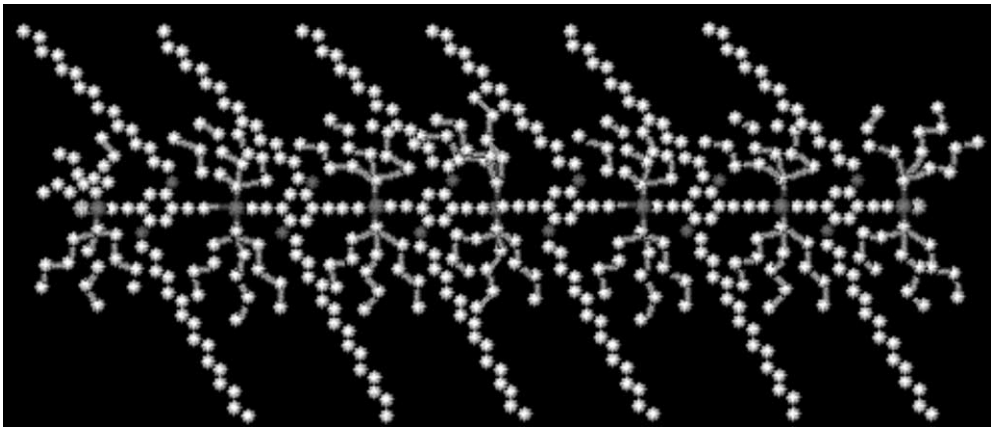

Fig. 6. Chemical structure of Pt–B–HDOB7.

The correlation between chemical structures and optical characteristics was assessed. Absorption spectra and luminescence quantum yields were correlated with the chain length, the nature of organic spacers and ancillary phosphines. Longer chains show red shift of the absorption maxima, and longer alkyl groups enhance the photoemission of the materials. Enhancement of charge density of the Pt atoms, flowing from the organic spacers, was also detected by XPS measurements, suggesting electron communication along the molecular backbone.

4. Experimental

4.1. General procedures

FTIR spectra were recorded as nujol mulls by using CsI cells, on a Perkin–Elmer 1700X Fourier Transform spectrometer. Multiple internal reflection spectra were performed by the same spectrometer as films deposited by $CHCl_3$ solutions on a TlI crystal recording the spectra at 60°. ^1H and ^{31}P-NMR spectra were recorded on a Bruker AC 300P spectrometer at 300 and 121 MHz, respectively, in appropriate solvents ($CDCl_3$, C_6D_6); the chemical shifts (ppm) were referenced to TMS for ^1H-NMR assigning the residual ^1H impurity signal in the solvent at 7.24 ppm ($CDCl_3$). The ^{31}P-NMR chemical shifts are relative to H_3PO_4 (85%). UV–vis spectra were recorded on Perkin-Elmer Lambda 16 instrument. PL spectra were performed on a Perkin–Elmer LS 50 Fluorescence Spectrometer. All measurements were performed at room temperature using quantitative solutions of the oligomers in $CHCl_3$ or thin films spin casted onto glass substrates by a commercial spinner. The molar extinction coefficient ε_o (with respect to the repeating unit) and the relative quantum yield η of both chloroform solutions and thin films were also determined. We adopted as the standard a solution of coumarine in ethanol ($c = 0.0028$ g l^{-1}), with a quantum yield equal to 51%, calculated by comparison with a rhodamine 6G solution ($c = 0.016$ g l^{-1}, $\eta = 90\%$) [56] as described below.

Quantitative solutions of coumarine and of oligomers were prepared on purpose, with the same absorbance at the excitation wavelength $\lambda_{max} = 350$ nm. The relative quantum yields were calculated from the measurements of the emission intensities of the sample and of the standard, considering the relationship: $\eta_{sample} = (I_{sample}/I_{standard}) \times \eta_{standard}$. All the data were corrected by taking into account the photomultiplier efficiency of the fluorescence spectrometer.

Molecular weights were determined by GPC on a Perkin–Elmer instrument equipped with a PL-gel column and UV detector. Measurements were performed in $CHCl_3$ (HPLC grade), using monodisperse polystyrene standards at 25 °C, flow rate 1 ml min^{-1}.

Elemental analyses were performed at the Department of Chemistry, University of Rome 'La Sapienza'.

XPS spectra were obtained using a custom designed spectrometer. A nonmonochromatised Mg–K_α X-rays source (1253.6 eV) was used and the pressure in the instrument was maintained at 1×10^{-9} Torr throughout the analysis. The experimental apparatus consists of an analysis chamber and a preparation chamber separated by a gate valve. An electrostatic hemispherical analyser (radius 150 mm) operating in the fixed analyser transmission mode and a 16-channel detector were used. The film samples were prepared by dissolving our materials in $CHCl_3$ and spinning the solutions onto polished stainless steel substrates. The samples showed good stability during the XPS analysis, preserving the same spectral features and chemical composition. BE were corrected by adjusting the position of the C1s peak to 285.0 eV in those samples containing mainly aliphatic carbons and to 284.7 eV in those containing more aromatic carbon atoms, in agreement with literature data [57].

The C1s, O1s, Pt4f, P2p, Cl2p and Sn3d spectra were deconvoluted into their individual peaks using the *Peak Fit* curve fitting program for PC.

Quantitative evaluation of the atomic ratios was obtained by analysis of the XPS signal intensity, employing Scofield's atomic cross-section values [58] and experimentally determined sensitivity factors.

All reactions were performed under an inert argon atmosphere using standard Schlenk glassware. Solvents were freshly degassed, dried by standard procedures and saturated with argon before use. Chromatographic separations were obtained with 70–230 mesh alumine (Merck), by using the appropriate eluents. The compounds 1,4-diiodo-2,5-bis(butyloxy)benzene and 1,4-diiodo-2,5-bis(hexadecyloxy) benzene were prepared by using the method described by Li [59] and used to prepare in situ the organic spacers 1,4-diethynyl-2,5-bis(butyloxy)benzene (BOB) and 1,4-diethynyl-2,5-bis(hexadecyloxy)benzene (HDOB). DEB was prepared by following a literature method [60]. Platinum complexes *cis*-[dichlorobis(triphenylphosphine)platinum(II)] and *trans*-[dichlorobis(tributylphosphine)platinum(II)] were prepared by reported methods [61].

4.2. Synthesis: general preparation of metal poly-ynes—$[ML_2(-C\equiv C-pC_6H_4(2,5OR)_2-C\equiv C-)]_n$

4.2.1. EOP reaction, method (a)

The following procedure for the preparation of Pt–B–HDOB*n* is representative of Pt–B–BOB*n*, Pt–P–BOB*n*, Pt–P–HDOB*n* and Pt–B–DEB*n*. The synthetic procedure is based on the 'EOP' method. In a Schlenk vessel 712 mg (0.88 mmol) of 1,4-diiodo-2,5-dihexade-

ciloxybenzene were introduced in 40 ml of THF in the presence of 100 mg (0.08 mmol) of [tetrakis(triphenylphosphine)palladium(0)]. Several vacuum/argon cycles were performed and then 552 mg (1.754 mmol) of tributyl(ethynyl)tin were added. The reaction mixture was heated at 70 °C for 15 h, until ^{1}H-NMR analysis indicated the complete consumption of the tin reagent. After cooling to 0 °C, 1.14 ml (2.28 mmol) of LDA were introduced. After 10 min the reaction was allowed to warm up and to reach room temperature. ^{1}H-NMR analysis indicated the complete transformation of the alkyne moieties into the tributyltin alkynyl functionalities. At this point, 559 mg (0.833 mmol) of *trans*-[dichlorobis-(tributylphosphine)platinum(II)] and 50 mg (0.044 mmol) of [dibenzilideneacetonepalladium(0)] were added, then the temperature was raised up to 70 °C, and the reaction was refluxed for 24 h. After cooling, the final reaction mixture was filtered through celite to eliminate the catalyst, the solvent volume of the filtrate was reduced to small volume and pentane was added to precipitate the polymeric material. With this procedure a red oily product, (Pt–B–HDOB*n*), was obtained.

4.2.2. Dehydrohalogenation reaction, method (b)

0.8 mmol of 1,4 bis(ethynyl)benzene and an equimolar amount of the square planar complex *trans*-[$Pt(PBu_3)_2Cl_2$] were added in the reaction flask in the presence of argon-bubbled diethylamine as solvent and base (30 ml). CuI was then added as catalyst (5% in mol) and the reaction allowed to react for 12 h at 55 °C. Ammonium salts were then removed by filtration and the residual dark brown solution reduced in volume. By adding methanol a brown powder (Pt–B–DEB*n*) was formed and then filtered.

The crude products prepared either with method (a) or (b) were purified with column chromatography on alumine using pentane/dichloromethane in increasing polarity ratio. Oligomers with different chain length and chlorine or tributylstannane as terminal groups, as XPS and conventional spectroscopic analysis assessed, could be separated and characterised from the crude products obtained by method (a). The characterisation of oligomers and polymers are hereafter reported in the elution order. The main characterisations and molecular formulas are collected in Table 1.

4.3. Reaction between 1,4-diiodobenzene and trans-bis(tributylphosphine)platinum(II) with method (a): Pt–B–DEB3(a)

1,4-diiodobenzene (300 mg, 0.990 mmol) was dissolved in freshly distilled THF and 570 mg (1.82 mmol) of tributylethynyltin were added under Ar, followed by the catalyst [$Pd(PPh_3)_4$] (105 mg, 0.09 mmol). The temperature was risen up to 70 °C and after stirring for 18 h the reaction mixture was cooled at 0 °C and LDA 2 M poured in (1.24 ml, 2.35 mmol). After adding *trans*-bis(tributylphosphine)platinum(II) (630 mg, 0.94 mmol), the mixture was warmed up at 70 °C for 24 h, then the solution was allowed to cool at room temperature and reduced in volume under vacuum. Addition of pentane caused the precipitation of a brown powder (970 mg, 46% yield).

4.3.1. Characterisation

IR ν(C≡C): 2104, ν(Pt–Cl): 328 cm^{-1}; UV ($CHCl_3$): 373.8 nm; ^{1}H-NMR ($CDCl_3$ ppm): 7.08 (s 8H Ar–H), 2.13 (36H P–CH_2–), 1.55 (m 36H –CH_2), 1.41 (m 36H –CH_2), 0.89 (t 54H–CH_3 $J = 9.08$ Hz); ^{31}P-NMR ($CDCl_3$ ppm, $J(^{195}Pt–^{31}P)$ Hz): 3.50 (2362.0), 0.76 (2303.0) (intensity ratio = 1:2); Elemental analysis (%), found (calculated for the trinuclear structure $C_{92}H_{170}P_6Pt_3Cl_2$, pm 2118.32): C, 51.71 (52.16); H, 8.17 (8.09).

4.4. Reaction between 1,4-bis(ethynyl)benzene and trans-bis(tributylphosphine)platinum(II) with method (b): Pt–B–DEBn(b)

1,4 bis(ethynyl)Benzene (100 mg, 0.8 mmol) and *trans*-[$Pt(PBu_3)_2Cl_2$] (526 mg, 0.8 mmol) were dissolved in argon-bubbled diethylamine with CuI as catalyst (5% in mol) and the temperature was risen up to 55 °C for 12 h. After removing ammonium salts, the addition of methanol yields a brown powder (300 mg, 52% yield).

4.4.1. Characterization

IR ν(C≡C): 2100 cm^{-1}; UV ($CHCl_3$): 378.4 nm; ^{1}H-NMR ($CDCl_3$ ppm): 7.07 (s 4H Ar–H), 2.09 (m 12H P–CH_2–), 1.57 (m 12H –CH_2), 1.41 (q 12H –CH_2), 0.89 (t 18H–CH_3 $J = 9.00$ Hz); ^{31}P-NMR ($CDCl_3$ ppm, $J(^{195}Pt–^{31}P)$ Hz): 3.50 (2360.8); Elemental analysis (%), found (calculated for the repeating unit $C_{34}H_{58}P_2Pt$): C, 56.15 (56.42); H, 8.54 (8.08); GPC molecular weight (in $CHCl_3$): $M_w = 57000$, $M_n = 18000$, $P = 3.2$, $n \cong 80$.

4.5. Reaction between 1,4-diiodo-2,5-di(butoxy)benzene and trans-bis(tributylphosphine)platinum(II) with method (a): Pt–B–BOBn(a)

1,4-diiodo-2,5di(butoxy)benzene (745 mg, 1.58 mmol) and 1 g (3.17 mmol) of tributylethynyltin were dissolved in THF under Ar, followed by the catalyst [$Pd(PPh_3)_4$] (180 mg, 0.16 mmol). After stirring for 18 h at 70 °C, the reaction mixture was cooled at 0 °C and LDA 2 M was added (1.96 ml, 4.0 mmol). At this point *trans*-bis(tributylphosphine)platinum(II) (1 g, 1.50 mmol) was introduced in the reaction vessel and the mixture warmed up at 70 °C for 24 h. The solution was then allowed to cool at room temperature and reduced in

volume. With the addition of pentane to the solution, a red oil was separated (980 mg, 75% yield), and chromatographic separation gave three main products.

4.5.1. Characterisations

4.5.1.1. Pt–B–BOB2(a). IR ν(C≡C): 2104, ν(Pt–P): 457, ν(P–C): 394, 280,ν(Pt–Cl): 326 cm^{-1}; UV ($CHCl_3$): $\varepsilon_0 = 2.03 \times 10^4$ l mol^{-1} cm^{-1}; $\lambda_{max} = 368.0$ nm; luminescence ($CHCl_3$): $\lambda_{max} = 470.0$ nm, $\eta = 0.25\%$; ^{1}H-NMR ($CDCl_3$): 6.70 (s Ar–H), 3.87 (t O–CH_2–), 2.18 (m P–CH_2–), 1.54 (m –CH_2), 1.41 (m –CH_2), 0.88 (t –CH_3); ^{31}P-NMR ($CDCl_3$ ppm, $J(^{195}Pt–^{31}P)$ Hz): 0.92 (2313.7); 10% of the crude product; Elemental analysis (%), found (calculated for the binuclear structure $C_{66}H_{128}O_2P_4Pt_2Cl_2$ ppm, 1538.68): C, 51.58 (51.52); H, 8.49 (8.38).

4.5.1.2. Pt–B–BOB3(a). IR ν(C≡C): 2106, ν(C–Sn): 525, 540, ν(Pt–P): 457, ν(P–C): 394, 280,ν(Pt–Cl): 328 cm^{-1}; UV ($CHCl_3$): $\varepsilon_0 = 7.64 \times 10^4$ l mol^{-1} cm^{-1}; $\lambda_{max} = 377.0$ nm; luminescence ($CHCl_3$): $\lambda_{max} = 465$, 445 nm, $\eta = 0.35\%$; ^{1}H-NMR ($CDCl_3$ ppm): 6.69 (s Ar–H), 3.87 (t O–CH_2–), 2.16 (m P–CH_2–), 1.54 (m –CH_2), 1.41 (m –CH_2), 0.88 (t –CH_3); ^{31}P-NMR ($CDCl_3$ ppm, $J(^{195}Pt–^{31}P)$ Hz): 0.91 (2316.5), 0.99 (2314.1), (intensity ratio = 2:1); 40% of the crude product; Elemental analysis (%), found (calculated for the trinuclear structure $C_{156}H_{249}O_6P_6Pt_3SnCl$: C, 56.79 (56.58); H, 8.50 (8.57).

4.5.1.3. Pt–B–BOB4(a). IR ν(C≡C): 2104, ν(C–Sn): 525, 533, ν(Pt–P): 457, ν(P–C): 394 cm^{-1}; UV ($CHCl_3$): $\varepsilon_0 = 1.41 \times 10^5$ l mol^{-1} cm^{-1}; $\lambda_{max} = 389.0$ nm; luminescence ($CHCl_3$): $\lambda_{max} = 470.0$ nm, $\eta = 0.85\%$; ^{1}H-NMR ($CDCl_3$ ppm): 6.70 (Ar–H), 3.87 (O–CH_2–), 2.16 (m P–CH_2–), 1.54 (m –CH_2), 1.41 (m –CH_2), 0.88 (–CH_3); ^{31}P-NMR ($CDCl_3$ ppm, (J^{195}Pt-^{31}P) Hz): 0.94 (2316.5), 1.01 (2314.1), (intensity ratio = 1:1); 10% of the crude product; Elemental analysis (%), found (calculated for the tetranuclear structure $C_{210}H_{370}O_{10}P_8Pt_4Sn_2$: C, 58.98 (58.38); H, 8.52 (8.63).

4.6. Reaction between 1,4-diiodo-2,5-di(butoxy)benzene and trans-bis(triphenylphosphine)platinum(II) with method (a): Pt–P–BOBn(a)

To 900 mg of 1,4-diiodo-2,5di(butoxy)benzene (1.91 mmol), dissolved in THF, 1.196 g (3.80 mmol) of tributylethynyltin were added under Ar, followed by the catalyst [$Pd(PPh_3)_4$] (88 mg, 0.07 mmol). After stirring at 70 °C for 18 h, the reaction mixture was cooled at 0 °C and LDA 2 M added (2.47 ml, 5.0 mmol). *Cis*-bis(triphenylphosphine)platinum(II) (1.425 g, 1.88 mmol) was then introduced into the vessel and the mixture warmed up at 70 °C for 24 h. At this point the solution was left to cool at room temperature and the volume reduced in vacuum. Addition of pentane allowed the separation of a red oil (1.36 g, 73% yield), whose chromatographic separation gave two main products.

4.6.1. Characterisation

4.6.1.1. Pt–P–BOB4(a). IR ν(C≡C): 2104, ν(C–Sn): 525, 533; 394, 280 cm^{-1}; UV ($CHCl_3$): $\varepsilon_0 = 3.46 \times 10^4$ l mol^{-1} cm^{-1}; $\lambda_{max} = 396.0$ nm; luminescence ($CHCl_3$): $\lambda_{max} = 440$, 460 nm, $\eta = 0.30\%$; ^{1}H-NMR ($CDCl_3$ ppm): 7.72 (m P–Ar–H), 7.35 (m P–Ar–H) 6.56 (Ar–H), 3.75 (t O–CH_2–), 2.09, 1.59 (m –CH_2), 1.35 (m –CH_2), 0.90 (m –CH_3); ^{31}P-NMR ($CDCl_3$ ppm, $J(^{195}Pt–^{31}P)$ Hz): 18.07 (2654.0), 17.67 (2610.0), (intensity ratio = 1:1); 40% of the crude product; Elemental analysis (%), found (calculated for the tetranuclear structure $C_{258}H_{274}O_{10}P_8Pt_4Sn_2$: C, 63.95 (64.55); H, 5.74 (5.75).

4.6.1.2. Pt–P–BOB2(a). IR ν(C≡C): 2104, ν(C–Sn): 525, 533; 279 cm^{-1}; UV ($CHCl_3$): $\varepsilon_0 = 1.96 \times 10^4$ l mol^{-1} cm^{-1}; $\lambda_{max} = 389.0$ nm; luminescence ($CHCl_3$): $\lambda_{max} = 470$ nm, $\eta = 0.11\%$; ^{1}H-NMR ($CDCl_3$ ppm): 7.72 (m P–Ar–H), 7.35 (m P–Ar–H) 6.56 (Ar–H), 3.75 (t O–CH_2–), 2.05 (s), 1.59 (m –CH_2), 1.35 (m –CH_2), 0.90 (m –CH_3); ^{31}P-NMR ($CDCl_3$ ppm, $J(^{195}Pt–^{31}P)$ Hz): 12.00 (3454.0); 10% of the crude product; Elemental analysis (%), found (calculated for the structure $C_{150}H_{174}O_6P_4Pt_2Sn_2$: C, 63.00 (63.78); H, 5.60 (6.20).

4.7. Reaction between 1,4-diiodo-2,5-di(butoxy)benzene and trans-bis(triphenylphosphine)platinum(II) with method (b): Pt–P–BOBn(b)

1,4-bis(ethynyl)-2,5di(butoxy)benzene (434 mg, 0.92 mmol) and *cis*-[$Pt(PPh_3)_2Cl_2$] (723 mg, 0.92 mmol) were dissolved in argon-bubbled diethylamine with CuI as catalyst (5% in mol) and the temperature was risen up to 55 °C for 12 h. After removing the ammonium salts, the addition of methanol yielded a red oil (500 mg, 55% yield).

4.7.1. Characterisation

4.7.1.1. Pt–P–BOBn(b). IR ν(C≡C): 2099 cm^{-1}; UV ($CHCl_3$): 370.2 nm; ^{1}H-NMR ($CDCl_3$): 7.72 (m P–Ar–H), 7.35 (m P–Ar–H) 6.93 (Ar–H), 3.96 (t O–CH_2–), 1.61 (m –CH_2), 1.38 (m –CH_2), 0.93 (m –CH_3), 0.86 (m –CH_3); ^{31}P-NMR ($CDCl_3$ ppm, $J(^{195}Pt–^{31}P)$ Hz): 18.18 (2682.0), 17.67 (2610.0) (intensity ratio 5:1); Elemental analysis (%), found (calculated for the repeating unit $C_{54}H_{50}O_2P_2Pt$): C, 66.12 (65.64); H, 5.13 (5.10); GPC molecular weight (in $CHCl_3$): $M_w = 7700$, $M_n = 3200$, $P = 2.4$, $n = 8–3$.

4.8. Reaction between 1,4-diiodo-2,5-di(hexadecyloxy)benzene and trans-bis(tributylphosphine)platinum(II) with method (a): Pt–B–HDOBn(a)

To a THF solution of 1,4-diiodo-2,5di(hexadecyloxy)benzene (712 mg, 0.88 mmol), 552 mg (1.754 mmol) of tributylethynyltin were added under Ar, followed by $[Pd(PPh_3)_4]$ (100 mg, 0.08 mmol). After stirring 18 h at 70 °C, the reaction mixture was cooled at 0 °C and 1.14 ml (2.28 mmol) of LDA 2 M were added. *Trans*-bis(tributylphosphine)platinum(II) (559 mg, 0.833 mmol) was then introduced and the mixture warmed up at 70 °C for 24 h. At this point the solution was allowed to cool at room temperature and reduced in volume. Addition of pentane allowed the separation of a red oil (720 mg, 72% yield), whose chromatographic separation gave two main products.

4.8.1. Characterisation

4.8.1.1. Pt–B–HDOB4(a). IR ν(C≡C): 2104, ν(Pt–Cl): 327, ν(Pt–P): 415 cm^{-1}; UV ($CHCl_3$): $\varepsilon_0 = 5.30 \times 10^4$ l mol^{-1} cm^{-1}; $\lambda_{max} = 377.0$ nm; luminescence ($CHCl_3$): $\lambda_{max} = 450$, 427 nm, $\eta = 2.33\%$; ^{1}H-NMR ($CDCl_3$ ppm): 6.69 (Ar–H), 3.73 (t O–CH_2–), 2.15 (m –CH_2), 1.65 (m –CH_2), 1.41 (m –CH_2), 0.88 (m –CH_3); ^{31}P-NMR ($CDCl_3$ ppm, $J(^{195}Pt-^{31}P)$ Hz): 0.90 (2300.0), 0.99 (2311.4), (intensity ratio = 1:1); Elemental analysis (%), found (calculated for the tetranuclear structure $C_{222}H_{420}O_6P_8Pt_4Cl_2$: C, 63.00 (62.23); H, 9.70 (9.88).

4.8.1.2. Pt–B–HDOB7(a). IR ν(C≡C): 2109, ν(Pt–Cl): 327, ν(Pt–P): 415 cm^{-1}; UV ($CHCl_3$): $\varepsilon_0 = 6.38 \times 10^5$ l mol^{-1} cm^{-1}; $\lambda_{max} = 380.0$ nm; luminescence ($CHCl_3$): $\lambda_{max} = 460$, 430 nm, $\eta = 3.16\%$; ^{1}H-NMR ($CDCl_3$ ppm): 6.69 (Ar–H), 3.75 (t O–CH_2–), 2.16 (m –CH_2), 1.55 (m –CH_2), 1.41 (m –CH_2), 0.90 (m –CH_3); ^{31}P-NMR ($CDCl_3$ ppm, $J(^{195}Pt-^{31}P)$ Hz): 0.90 (2300.0), 1.00 (2311.4), (intensity ratio = 2:5); Elemental analysis (%), found (calculated for the heptanuclear structure $C_{420}H_{786}O_{12}P_{14}Pt_7Cl_2$: C, 64.02 (63.86); H, 9.91 (10.03).

4.9. Reaction between 1,4-diiodo-2,5-di(hexadecyloxy)benzene and cis-bis(triphenylphosphine)platinum(II) with method (a): Pt–P–HDOBn(a)

712 mg of 1,4-diiodo-2,5di(hexadecyloxy)benzene (0.88 mmol) and 552 mg (1.754 mmol) of tributylethynyltin were mixed in THF under Ar; the catalyst $[Pd(PPh_3)_4]$ (100 mg, 0.08 mmol) was then introduced in the reaction vessel and after stirring the mixture for 18 h at 70 °C, the reaction was cooled at 0 °C. LDA 2 M was added (1.14 ml, 2.28 mmol), followed by *cis*-bis(triphenylphosphine)platinum(II) (659 mg, 0.833 mmol) and the mixture was warmed up to 70 °C for 24 h. The solution was then cooled at room temperature and reduced in volume. Addition of pentane led to the separation of a red oil (880 mg, 80% yield). In this case, no chromatographic separation was performed, and the oily product was characterised.

4.9.1. Pt–P–HDOBn(a)

IR ν(C≡C): 2106 cm^{-1}; UV ($CHCl_3$): $\varepsilon_0 = 3.00 \times 10^5$ l mol^{-1} cm^{-1}; $\lambda_{max} = 371.2$ nm; luminescence ($CHCl_3$): $\lambda_{max} = 450$, 440 nm, $\eta = 0.34\%$; ^{1}H-NMR ($CDCl_3$, δ ppm): 7.7 (m 18H, *phosphine*), 7.4 (m 12H, *phosphine*), 6.65 (m 2H, Ar–*H*), 3.98 (t 4H, O–CH_2–), 1.55–1.41 (m 56H, –CH_2–), 0.90 (m 6H, –CH_3); ^{31}P-NMR ($CDCl_3$ ppm, $J(^{195}Pt-^{31}P)$ Hz): 18.00 (2595.0); Elemental analysis (%), found (calculated for the repeating unit $C_{78}H_{78}O_2P_2Pt$): C, 71.20 (70.72); H, 7.31 (7.46); GPC molecular weight (in $CHCl_3$): $M_w = 26700$, $M_n = 15800$ $P = 1.7$.

Acknowledgements

The authors gratefully acknowledge Prof. Claudio Lo Sterzo for helpful discussions. This work was financially supported by CNR (Italy), Progetto Finalizzato MSTA2.

References

[1] (a) R.P. Kingsborough, T.M. Swager, Transition metal coordination in polymeric (π-conjugated organic frameworks, in: K.D. Karlin (Ed.), Progress in Inorganic Chemistry, vol. 48, Wiley, New York, 1999, p. 123;
(b) C. Huber, F. Bangerter, W.R. Caseri, C. Weder, J. Am. Chem. Soc. 123 (2001) 3857.
[2] F.Q. Liu, G. Harder, T.D. Tilley, J. Chem. Am. Soc. 120 (1998) 3271.
[3] S. Takahashi, E. Murata, M. Kariya, K. Sonogashira, N. Hagihara, Macromolecular 12 (1979) 1016.
[4] N.J. Long, Angew. Chem. Int. Ed. Engl. 34 (1995) 21.
[5] W.J. Blau, H.J. Byrne, D.J. Cardin, A.P. Davey, J. Mater. Chem. 1 (1991) 245.
[6] N. Hagihara, K. Sonogashira, S. Takahashi, Adv. Polym. Sci. 41 (1981) 151.
[7] N. Chawdhury, A. Kohler, R.H. Friend, M. Younus, N.J. Long, P.R. Raytby, J. Lewis, Macromolecular 31 (1998) 722.
[8] M. Hmyene, A. Yassar, M. Escorne, F. Garnier, Adv. Mater. 6 (1994) 564.
[9] G. Tormos, P. Nugara, M.V. Lakshmikantham, M.P. Cava, Synth. Metab. 53 (1993) 271.
[10] M. Bochmann, K. Kelly, J. Chem. Soc. Chem. Commun. (1989) 532.
[11] M. Younus, A. Kohler, S. Cron, N. Chawdhurry, M.R.A. Al-Mandhary, M.S. Khan, J. Lewis, N.J. Long, R.H. Friend, P.R. Raithby, Angew. Chem. Int. Ed. 37 (1998) 3036.
[12] J. Lewis, M.S. Khan, S.J. Davies, A.K. Kakkar, B.F. Johnson, T.B. Marder, H.B. Fyfe, F. Wittmann, R.H. Friend, A.E. Dray, J. Organomet. Chem. 425 (1992) 165.

[13] M.C.B. Colbert, J. Lewis, N.J. Long, P.R. Raithby, M. Younus, A.J.P. White, D.J. Williams, N.J. Payne, L. Yellowless, D. Beljonne, N. Chawdhurry, R.H. Friend, Organometallics 17 (1998) 3034.
[14] D.L. Lichtenberger, S.K. Renshaw, R.M. Bullock, J. Am. Chem. Soc. 115 (1993) 3276.
[15] H.F. Wittmann, K. Fuhrmann, R.H. Friend, M.S. Khan, J. Lewis, Synth. Metab. 55–57 (1993) 56.
[16] V. Belluco, R. Bertani, R.A. Michelin, M. Mozzon, J. Organomet. Chem. 600 (2000) 37.
[17] M.S. Khan, A.K. Kakkar, N.J. Long, J. Lewis, P. Raithby, P. Nguyen, T.B. Marder, F. Wittmann, R.H. Friend, J. Mater. Chem. 4 (1994) 1227.
[18] W.Y. Wong, G.L. Lu, K.H. Choi, J.X. Shi, Macromolecular 35 (2002) 3506.
[19] P. Altamura, G. Giardina, C. Lo Sterzo, M.V. Russo, Organometallics 20 (2001) 4360.
[20] M.S. Khan, M.R.A. Al-Mandhary, M.K. Al-Suti, N. Feeder, S. Nahar, A. Köhler, R.H. Friend, P.J. Wilson, P.R. Raithby, J. Chem. Soc. Dalton Trans. (2002) 2441.
[21] (a) G. Frapper, M. Kertesz, Inorg. Chem. 32 (1993) 732;
(b) N. Re, A. Sgamellotti, C. Floriani, J. Chem. Soc. Dalton Trans. (1998) 2521.
[22] K. Sonogashira, S. Takahashi, N. Hagihara, Macromolecular 10 (1977) 879.
[23] N. Hagihara, K. Sonogashira, S. Takahashi, Adv. Polym. Sci. 41 (1981) 151.
[24] S. Takahashi, M. Karija, T. Yatake, K. Sonogashira, N. Hagihara, Macromolecular 11 (1978) 1063.
[25] S.J. Davies, B.F.G. Johnson, M.S. Khan, J. Lewis, J. Chem. Soc. Chem. Commun. (1991) 187.
[26] M.S. Khan, A.K. Kakkar, N.J. Long, J. Lewis, P. Raithby, P. Nguyen, T.B. Marder, F. Wittmann, R.H. Friend, J. Mater. Chem. 4 (1994) 1227.
[27] J. Lewis, P.R. Raithby, W.Y. Wang, J. Organomet. Chem. 556 (1998) 219.
[28] J. Lewis, M.S. Khan, A.K. Kakkar, B.F.G. Johnson, T.B. Marder, H.B. Fyfe, F. Wittmann, R.H. Friend, A.E. Day, J. Organomet. Chem. 425 (1992) 165.
[29] D. Beljonne, H.F. Wittmann, A. Kohler, S. Graham, M. Younus, J. Lewis, P.R. Raithby, M.S. Khan, R.H. Friend, J.L. Bredas, J. Chem. Phys. 105 (1996) 3868.
[30] J.K. Stille, Angew. Chem. Int. Ed. Engl. 25 (1986) 508.
[31] C. Lo Sterzo, J.K. Stille, Organometallics 9 (1990) 687.
[32] E. Antonelli, P. Rosi, C. Lo Sterzo, E. Viola, J. Organomet. Chem. 578 (1999) 210.
[33] G. Giardina, P. Rosi, A. Ricci, C. Lo Sterzo, J. Polym. Sci. (A): Polym. Chem. 38 (2000) 2603.
[34] R. Crescenzi, C. Lo Sterzo, Organometallics 11 (1992) 4301.
[35] A. Buttinelli, E. Viola, E. Antonelli, C. Lo Sterzo, Organometallics 17 (1998) 2574.
[36] C. Caliendo, I. Fratoddi, M.V. Russo, Appl. Phys. Lett. 80 (2002) 4849.
[37] C. Caliendo, I. Fratoddi, C. LoSterzo, M.V. Russo, J. Appl. Phys., in press.
[38] N.J. Long, A.J. Martin, R. Vilar, A.J.P. White, D.J. Williams, M. Younus, Organometallics 18 (1999) 4261.
[39] D. Osella, R. Gobetto, C. Nervi, M. Ravera, R. D'Amato, M.V. Russo, Inorg. Chem. Commun. 1 (1998) 239.
[40] A. Furlani, S. Licoccia, M.V. Russo, A. Chiesi Villa, C. Guastino, J. Chem. Soc. Dalton Trans. (1984) 2197.
[41] K.S. Kwok, J.C. Ellenbogen, Mater. Today 5 (2002) 28.
[42] X.A. Guo, K.C. Sturge, A.D. Hunter, M.C. Williams, Macromolecular 27 (1994) 7925.
[43] K.A. Walters, L.L. Premvardhan, Y. Liu, L.A. Peteanu, K.S. Schanze, Chem. Phys. Lett. 339 (2001) 255.
[44] A.E. Dray, F. Wittmann, R.H. Friend, A.M. Donald, M.S. Khan, J. Lewis, B.F.G. Johnson, Synth. Metab. 41–43 (1991) 871.
[45] R.D. Markwell, I.S. Butler, A.K. Kakkar, M.S. Khan, Z.H. Al-Zakwam, J. Lewis, Organometallics 15 (1996) 2331.
[46] H.F. Wittmann, K. Fuhrmann, R.H. Friend, M.S. Khan, J. Lewis, Synth. Metab. 55–57 (1993) 56.
[47] A. Kohler, H.F. Wittmann, R.H. Friend, M.S. Khan, J. Lewis, Synth. Metab. 77 (1996) 147.
[48] W.Y. Wong, K.H. Choi, G.L. Lu, J.X. Shi, Macromol. Rapid Commun. 22 (2001) 461.
[49] N. Chawdhury, A. Köhler, R.H. Friend, W.Y. Wong, J. Lewis, M. Younus, P.R. Raithby, T.C. Corcoran, M.R.A. Al-Mandhary, M.S. Khan, J. Chem. Phys. 110 (1999) 4963.
[50] G. Polzonetti, V. Faruffini, A. Furlani, M.V. Russo, Synth. Metab. 29 (1989) E495.
[51] G. Iucci, G. Infante, G. Polzonetti, Polymer 43 (2002) 655.
[52] G. Polzonetti, A. Ferri, M.V. Russo, G. Iucci, S. Licoccia, R. Paolesse, J. Vac. Sci. Technol. A 17 (1999) 832.
[53] D.T. Clark, D.B. Adams, D. Briggs, Chem. Commun. (Cambridge) (1971) 602.
[54] V.J. Nefedov, Ya.V. Salyn, Inorg. Chim. Acta 28 (1978) L135.
[55] Host, J. Electrospectroscopy Relat. Phenom. 5 (1974) 227.
[56] O. Svelto, Principles of Lasers (Chapter 6), Plenum Press, NewYork, 1989.
[57] G. Beamson, D. Briggs, High Resolution XPS of Organic Polymers, the Scienta ESCA300 Database, Wiley, New York, 1992.
[58] J.M. Scofield, J. Electron Spectrosc. Relat. Phenom. 8 (1976) 129.
[59] H. Li, D.R. Powell, R.K. Hayashi, R. West, Macromolecular 31 (1998) 52.
[60] (a) S. Takahashi, Y. Kuroyama, K. Sonogashira, N. Hagihara, Synthesis (1980) 627;
(b) R. Nast, H. Grouhi, J. Organomet. Chem. 182 (1979) 197.
[61] (a) G.B. Kaufmann, L.A. Teter, Inorg. Synth. 7 (1963) 245;
(b) F.R. Hartley, Coord. Chem. Rev. 41 (1982) 319;
(c) P.G. Leviston, M.G. Wallbridge, J. Organomet. Chem. 110 (1976) 271;
(d) J. Chatt, R.G. Hayter, J. Chem. Soc. Dalton Trans. (1961) 896.